# Design of Flux-switching DC-field Machines with Harmonics Suppression

**Libing Cao [1], K. T. Chau [1], Christopher H. T. Lee [2], C. C. Chan [1] and T. W. Ching [3]**

*1)Dept. of Electrical and Electronic Engineering,*

*The University of Hong Kong, Hong Kong, China (E-mail: ktchau@eee.hku.hk)*

*2) Research Laboratory of Electronics,*

*Massachusetts Institute of Technology, Cambridge, USA*

*3) Faculty of Science and Technology,*

*University of Macau, Macau, China*

Presented at EVS 31 & EVTeC 2018, Kobe, Japan, October 1-3, 2018

**ABSTRACT**: This paper proposes and analyzes a design approach for flux-switching DC-field (FSDC) machines with harmonics suppression. By purposely selecting appropriate stator/rotor-pole combinations, the even harmonics of phase coils can be cancelled and hence the harmonics suppression of back electromotive force (EMF) of the phase winding. The design criteria are firstly derived from the view of slot star diagram and back-EMF vectors, based on which the mathematics conditions are established. Then, the FSDC machines are optimized by multi-objective genetic algorithm (MOGA) coupled with finite-element analysis (FEA) under the fixed copper loss. Consequently, the back-EMF harmonics of the phase winding and coils of the optimized machines are analyzed by FEA. It shows that the even harmonics of back-EMF of phase coils can be cancelled and the phase winding total harmonic distortion (THD) is significantly suppressed by the proposed method.

**KEY WORDS**: Flux-switching DC-field machines, harmonics suppression, optimization, total harmonic distortion (THD)

## 1. INTRODUCTION

With ever-increasing concern on the energy utilization and environmental protection, electric vehicles (EVs) have received great attention and rapid development [1-3]. As the core technology of EVs, electric machines are generally required to operate with high torque density, high efficiency, wide speed range, high reliability and robustness, and reasonable cost [4-6]. Among them, the stator-PM machines especially the flux-switching permanent magnet (FSPM) machine have achieved most of the criteria [7-9]. However, FSPM machines generally suffer from several problems due to the usage of rare-earth PM materials, which are complex flux-regulation algorithm, potential PM demagnetization threat, and low cost-effectiveness. To improve these problems, flux-switching DC-field (FSDC) machines are developed with the installation of independent DC excitation windings [10-12]. Meanwhile, in order to operate in brushless AC (BLAC) mode with lower torque ripple than BLDC mode, the back electromotive force (EMF) waveforms are expected to be sinusoidal [13-15]. Hence, it is necessary to analyze and suppress the harmonics of the back EMF of FSDC machines. Although the back-EMF of FSPM machines with flux-focusing topology has been investigated in [16-18], the back EMF of FSDC machine and its harmonics still remain to be analyzed.

This paper proposes and analyzes a design approach for FSDC machines with harmonics suppression. By purposely selecting appropriate numbers of stator and rotor poles, the even harmonics of phase coils can be cancelled and hence the harmonics suppression of back EMF of the phase winding. The paper is presented as follows. In Section 2, the design criteria and mathematics conditions are derived from the view of slot star diagram and back-EMF vectors. For exemplification, two three-phase FSDC machines (see Fig. 1) with different stator and rotor pole combinations, namely 12-stator poles and 7-rotor poles (12s/7r) and 12-stator poles and 8-rotor poles (12s/8r) are initially designed. In Section 3, the two FSDC machines are optimized by multi-objective genetic algorithm (MOGA) coupled with finite-

element analysis (FEA) under the same copper loss. The electromagnetic performances are also compared including steady torque, torque ripple and efficiency. In Section 4, the back-EMF harmonics of the optimized machines are analyzed, followed by the conclusions in Section 5.

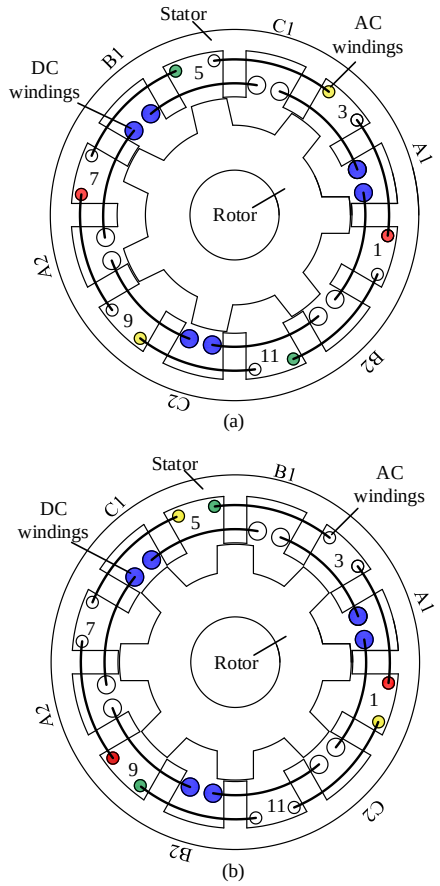


Fig. 1. 12s/7r and 12s/8r FSDC machines. (a) Proposed 12s/7r machine. (b) Conventional 12s/8r machin**e**

## 2. DESIGN CRITERIA

### 2.1. Machine Structure

Fig. 1 shows the structures of proposed 12s/7r and conventional 12s/8r FSDC machines, which both comprise an inner rotor and outer stator. Instead of adopting the toroidal-field topology, the machines utilize the wound-field winding configuration here since it takes the advantage of smaller flux leakage over the toroidal-field counterpart, in which the DC-field flux close to stator outer surface will not goes through the rotor but outside of the stator. Besides, the inner stator consists of 12 stator poles, on which both DC-field and armature winding are wound in every other stator slot while the rotor is simply iron core with salient poles. Although these two machines share the same structure except for the number of the rotor poles, the slot/rotor poles combinations are different and hence determines the back-EMF characteristics, which will be illustrated later on.

### 2.2. Coil-EMF Vectors and Connections

Since the FSDC machine operates in the BLAC mode with lower torque ripple, the operation principle in essence is same as the permanent magnet synchronous machine (PMSM). Therefore, the slot-star diagrams of these two machines are firstly analyzed, based on which the coil connections for the 12s/7r and 12s/8r machines are formed in order to produce the sinusoidal three-phase back-EMF with 120 elec. degree displacement and hence the steady electromagnetic torque.

Fig. 2 shows the slot star diagram and phase coil diagram of the 12s/7r and 12s/8r FSDC machines. Based on the phase coil diagrams, the corresponding phase windings are connected as shown in Fig. 1. It should be noted that *n'* means the opposite polarity of the *n* due to the alternate DC excitation directions in the stator poles, for example, coil 1 and coil 3.

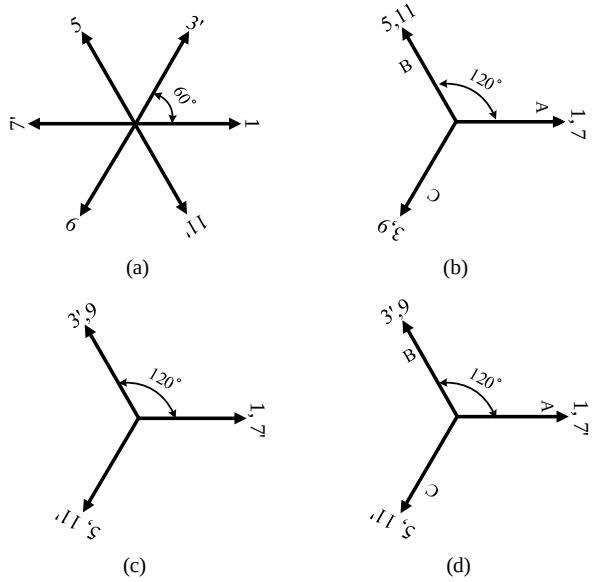


Fig. 2. Slot star diagram and phase coil diagram. (a) Slot star diagram of 12s/7r machine (electrical degree). (b) Phase coils diagram of 12s/7r machine. (c) Slot star diagram of 12s/8r machine (electrical degree). (d) Phase coils diagram of 12s/8r machine.

### 2.3 Mathematics Conditions

In order to illustrate the stator/rotor pole combination criteria, the coil back-EMF of the individual coils can be expressed as a periodic function against the rotor position:

$$\varphi(n,\theta_{0n}) = \sum_{n=1}^{\infty} \varphi_n e^{jnN_r(\omega t+\theta_{0n})} = \sum_{n=1}^{\infty} \varphi_n e^{jnN_r(\theta+\theta_{0n})} \quad (1)$$

in which $t$ , $\theta$ , $\omega$ , $\theta_{0n}$ ; $\varphi_n$ are the fundamental rotation time, rotation mechanical angle, mechanical angular speed and initial mechanical angle respectively; the amplitude of nth-order harmonics of coil back-EMF.

In the 12s/7r FSDC machine, taking the phase A coils for exemplification, coil A1 back -EMF can be expressed as (1) while coil A7 can be written as

$$\begin{aligned}\varphi(n,\theta_{0n}) &= \varphi(n,\theta_{0n}+\frac{\pi}{N_r})\cdot e^{j\pi} \\ &= \sum_{n=1}^{\infty}\varphi_n e^{jnN_r(\theta+\theta_{0n})}\cdot e^{j(n\pi+\pi)}\end{aligned} \tag{2}$$

in which the $e^{j\pi}$ is due to the alternate DC excitation directions in the stator poles. Based on the phase winding connection, coil A back-EMF can be deduced as (1) + (2), i.e.,

$$\varphi(n,\theta_{0n}) = \sum_{n=1}^{\infty}\varphi_n e^{jnN_r(\theta+\theta_{0n})}\cdot(1+e^{j(n\pi+\pi)}) \tag{3}$$

Thus, the even harmonics of back-EMF of phase winding A in 12s/7r machine can be cancelled theoretically, i.e.,

$$\varphi(\theta_{2n}) = 0 \tag{4}$$

Similarly, in the 12s/8r FSDC machine, coil A1 back -EMF can be expressed as (1) while coil A7 can be written as

$$\begin{aligned}\varphi(n,\theta_{0n}) &= \varphi(\theta_n+\frac{2\pi}{N_r})\cdot e^{j\pi} \\ &= \sum_{n=1}^{\infty}\varphi_n e^{jnN_r(\theta+\theta_{0n})}\cdot e^{j(2n\pi+\pi)}\end{aligned} \tag{5}$$

Based on the phase winding connection, coil A back-EMF can be deduced as (1) - (2), i.e.,

$$\varphi(n,\theta_{0n}) = \sum_{n=1}^{\infty}\varphi_n e^{jnN_r(\theta+\theta_{0n})}\cdot(1-e^{j(2n\pi+\pi)}) \tag{6}$$

Thus, the even harmonics of back-EMF of phase winding A in 12s/8r machine cannot be canceled theoretically due to

$$\varphi(n,\theta_{0n}) = 2\sum_{n=1}^{\infty}\varphi_n e^{jnN_r(\theta+\theta_{0n})} \tag{7}$$

To summarize, due to the 180 electrical degree displacement between the coils of one phase windings, the even harmonics can be cancelled in the resultant phase winding.

Based on the above analysis, the stator/rotor pole combinations of the proposed method are deduced as follows. The angular difference between two coils in any one phase is given by $2\pi N_r n_{spp} / N_s$ in elec. degree, where $n_{spp}$ is the number of stator pole pitch between the two coils. Therefore, in order to achieve the 180 electrical degree displacement between the coils of one phase windings, the following condition should be satisfied:

$$\frac{2\pi N_r n_{spp}}{N_s} = (2k\text{-}1)\pi \tag{8}$$

where k is a positive integer. Moreover, (8) can be rewritten as

$$\frac{N_r}{N_s} = \frac{(2k\text{-}1)}{2n_{spp}} = \frac{\text{odd numerator}}{\text{even denominator}} \tag{9}$$

Apparently, 12s/7r FSDC machine is one the special case of equation (9) with $N_r$ =7 and $N_s$ =12. Meanwhile, the proposed stator/slot combination criterion is different from the conventional one [1]:

$$\begin{cases} N_s = 2mi \\ N_r = N_s \pm 2j \end{cases} \tag{10}$$

where $N_s$ is the number of stator poles, $N_r$ is the number of rotor poles, $m$ is the number of phases of the armature windings, and $i$ and $j$ are positive integers. Therefore, 12s/8r FSDC machine is one the special case of equation (10) with $m$ =3, $i$ =2, $N_r$ =8 and $N_s$ =12.

Table 1 Constant Parameters of the 12s/7r and 12s/8r Machine

| Machine | 12s/7r | 12s/8r |
|---|---|---|
| Stator outside diameter (mm) | 124 | 124 |
| Rotor inside diameter (mm) | 30 | 30 |
| Air-gap length (mm) | 0.5 | 0.5 |
| Filling factor | 0.6 | 0.6 |
| Lamination factor | 0.98 | 0.98 |
| Axial length (mm) | 120 | 120 |
| Rotor poles | 7 | 8 |
| Stator poles | 12 | 12 |
| Current density (RMS, A/mm$^2$) | 6 | 6 |
| Number of turns of DC coil | 100 | 100 |
| Number of turns of AC coil | 100 | 100 |
| Copper loss (Including end winding, W) | 166 | 166 |
| Iron core material | 50JN700 | 50JN700 |
| Rated speed (rpm) | 300 | 300 |
| Operation temperature ($^0$C) | 20 | 20 |

## 3. DESIGN OPTIMIZATION

Since the back-EMF harmonics are not only influenced by the stator/rotor poles combination but also determined by the machine design parameters such as the stator/rotor pole arc ratios and pole heights, it is necessary to optimize the two machine design parameters in order to have a fair comparison before we conduct harmonics analysis in Section 4.

As we know, the torque ripple is mainly resulted from the cogging torque and especially the back-EMF harmonics or electromagnetic torque ripple. To simplify the optimization process, the back-EMF THD optimization can be indirectly equivalent to the torque ripple optimization. Besides, the steady torque value is the key electromagnetic performance of machine. Thus, the optimization objectives are the maximum steady torque and minimum torque ripple.

To achieve these aims, the 12s/7r and 12s/8r machines are optimized by utilizing the MOGA method coupled with FEA in the commercial JMAG-designer software. During the optimization process, the machine constant parameters and dimensions are listed in Table 1. Meanwhile, the variable parameters are indicated in Fig. 3 and denoted in Table 2. After the MOGA optimization under the same total copper loss, the optimized design parameters values are listed and compared in Table 3.

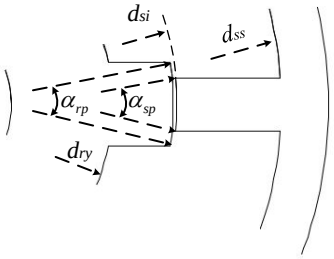


Fig. 3. Machine variable parameters

Table 2 Machine Variable Parameters

| Parameters | Symbols |
|---|---|
| Stator slot diameter (mm) | $d_{ss}$ |
| Stator inside diameter (mm) | $d_{si}$ |
| Rotor yoke diameter (mm) | $d_{ry}$ |
| Angle of stator pole (deg) | $\alpha_{sp}$ |
| Angle of rotor pole (deg) | $\alpha_{rp}$ |

Table 3 Initial and Optimized Parameter Values

| Machine | 12s/7r | | 12s/8r | |
|---|---|---|---|---|
| Parameters | Initial value | Optimized value | Initial value | Optimized value |
| $d_{ss}$ | 110 | 112.8 | 110 | 102.6 |
| $d_{si}$ | 79 | 75.8 | 79 | 73.8 |
| $d_{ry}$ | 60 | 50.8 | 60 | 53.9 |
| $\alpha_{sp}$ | 11.25 | 13.85 | 11.25 | 15.67 |
| $\alpha_{rp}$ | 18 | 20.42 | 18 | 20.75 |

Table 4 Initial and Optimized Electromagnetic Performances

| Machine | Initial | | Optimized | |
|---|---|---|---|---|
| | 12s7r | 12s8r | 12s7r | 12s8r |
| Steady torque (Nm) | 13.51 | 10.89 | 15.56 | 10.90 |
| Torque ripple | 0.20 | 1.13 | 0.068 | 0.29 |
| Rated speed (rpm) | 300 | 300 | 300 | 300 |
| Current density (A/mm$^2$) | 6 | 6 | 6 | 6 |
| Copper loss (Including end winding, W) | 166 | 166 | 166 | 166 |
| Iron loss (W) | 39.7 | 25.3 | 56.9 | 34.95 |
| Rated power (W) | 425 | 342 | 490 | 342 |
| Efficiency | 0.67 | 0.64 | 0.69 | 0.63 |

Fig. 4 shows the MOGA optimization results of the last two generations while Fig. 5 shows the steady torque of the corresponding selected optimized design including the initial design. Furthermore, Table 4 summarizes the initial and optimized electromagnetic performances. It can be seen that the torque ripple and steady torque is decreased by 66% and 15% in 12/7r machine, respectively while 74% and 0.1% in 12/8r machine, respectively. In addition, the efficiency maintains normal level about 65%-70%, which is relatively lower than that of the permanent-magnet counterpart due to the DC-field excitation.

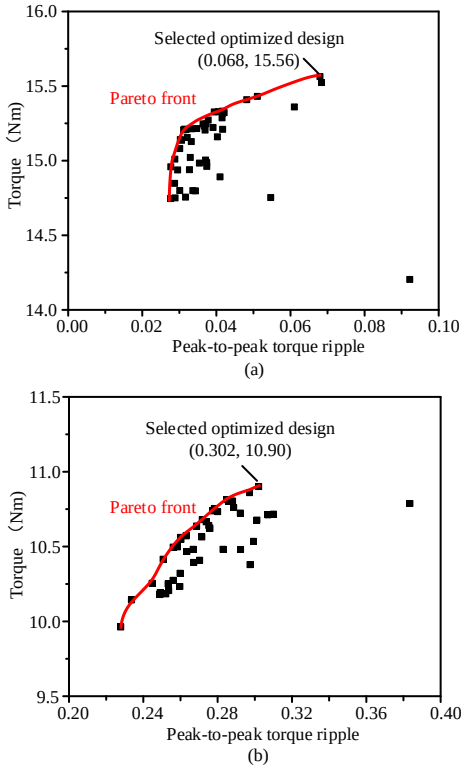


Fig. 4. MOGA optimization results of the last two generations. (a) 12s/7r machine. (b) 12s/8r machine.

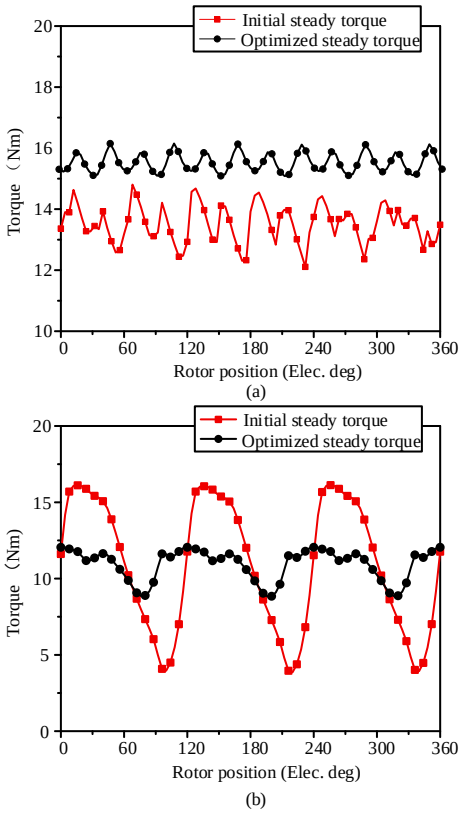


Fig. 5. Initial and optimized steady torque of machines. (a) 12s/7r machine. (b) 12s/8r machine.

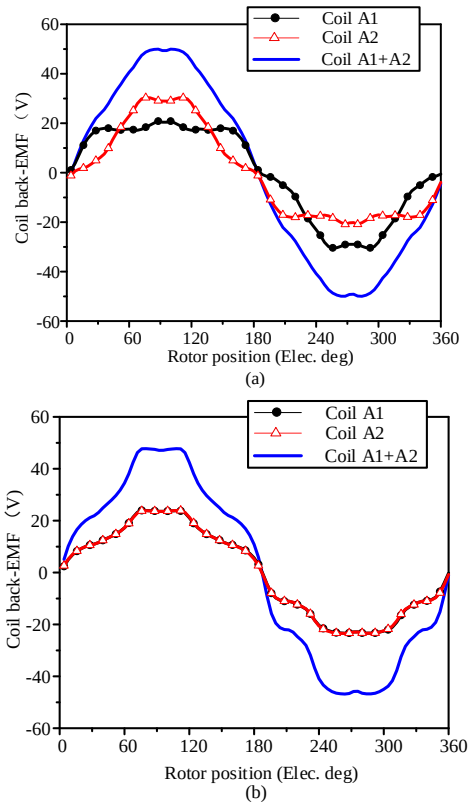


Fig. 6. Coil back-EMF of the optimized machines. (a) 12s/7r machine. (b) 12s/8r machine.

## 4. HARMONICS ANALYSIS

In order to verify the effectiveness of harmonics suppression of the slot/rotor pole selection principle as stated in Section 2, the back-EMF waveforms and their spectrum results of the two optimized 12s/7r and 12s/8r FSDC machines are analyzed and obtained by FEA and FFT, respectively.

Fig. 6 shows the coil back-EMF of phase A while Fig. 7 shows the corresponding harmonics spectrums. It should be noted that in Fig. 7 the harmonics percentages of individual coil A1, A2 and resultant phase coil A1+A2 refer to their corresponding fundamental component magnitudes. One can see that both in 12s/7r and 12s/8r machines the individual coil A1 and coil A2 of phase A are asymmetric due to their large even harmonics. However, the resultant A-phase back-EMF is symmetric and shows low THD due to the even harmonic cancellation in coil A1 and coil A2 in the 12s/7r machine. Meanwhile, although the even harmonics percentages of individual coils and resultant phase coil in 12s/8r machine keep almost the same level, the even harmonics magnitudes of the resultant phase coil are the twice of those of the individual coils due to the different reference values as stated earlier. These above FEA and FFT results well match the mathematical equations (4) and (7), thereby verifying the effectiveness of the proposed harmonics suppression method.

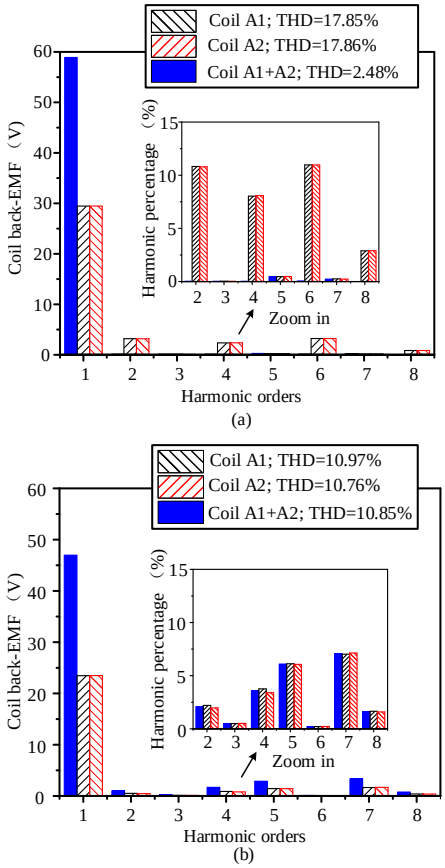


Fig. 7. Harmonic analysis of back-EMF of the optimized machines. (a) 12s/7r machine. (b) 12s/8r machine.

## 5. CONCLUSIONS

In this paper, an effective approach of the back-EMF harmonics suppression of FSDC machine is proposed from the view of the slot star diagram and coil-EMF vectors, based on which the mathematics conditions are given. In order to have a fair comparison of the conventional and proposed slot/rotor pole combination method, their corresponding FSDC machines are optimized by MOGA coupled with FEA method. The analytical and FEA results show that the even harmonics of back-EMF of phase coils can be cancelled and the phase winding THD is significantly suppressed by the proposed method. Meanwhile, the prototypes are in the process of manufacture and the experimental verification will be also given in the future.


## ACKNOWLEDGEMENTS

This work was supported by the Hong Kong Research Grants Council, Hong Kong Special Administrative Region, China [Project number 17200614].


## REFERENCES


(1) K. T. Chau. Electric vehicle machines and drives: design, analysis and application. 2015. New York, NY, USA: Wiley.

(2) K. T. Chau and W. Li. Overview of electric machines for electric and hybrid vehicles. International Journal of Vehicle Design. 2014. vol. 64, no. 1, pp. 46-71.

(3) Z. Q. Zhu and D. Howe. Electrical machines and drives for electric, hybrid, and fuel cell vehicles. Proceeding of IEEE. 2007. vol. 95, pp. 746-765.

(4) K. T. Chau, C. C. Chan, and C. Liu. Overview of permanent-magnet brushless drives for electric and hybrid electric vehicles. IEEE Transactions on Industrial Electronics. 2008. vol. 55, no. 6, pp. 2246-2257.

(5) K. T. Chau, C.Q. Jiang, W. Han, and C. H. T. Lee. State-of-the-art electromagnetics research in electric and hybrid vehicles. Progress in Electromagnetics Research. 2017. vol. 159, pp. 139-157.

(6) M. Cheng, W. Hua, J. Zhang, and W. Zhao. Overview of stator-permanent magnet brushless machines. IEEE Transactions on Industrial Electronics. 2011. vol. 58, no. 11, pp. 5087-5101.

(7) C. Liu, K. T. Chau, J. Z. Jiang, and S. Niu. Comparison of stator-permanent-magnet brushless machines. IEEE Transactions on Magnetics. 2008. vol. 44, no. 11, pp. 4405-4408.

(8) X. Zhu, K. T. Chau, M. Cheng, and C. Yu. Design and control of a flux-controllable stator-permanent magnet brushless motor drive. Journal of Applied Physics. 2008. vol. 103, no. 7, pp. 7F134:1-3.

(9) Z. Q. Zhu, Z. Z. Wu, D. J. Evans, and W. Q. Chu. A wound field switched flux machine with field and armature windings separately wound in double stators. IEEE Transactions on Energy Conversion. 2015. vol. 30, pp.772-783.

(10) Y. Fan and K. T. Chau. Design, modeling, and analysis of a brushless doubly fed doubly salient machine for electric vehicles. IEEE Transactions on Industry Applications. 2008. vol. 44, no. 3, pp. 727-734.

(11) Y. Tang, E. Ilhan, J. Paulides, and E. Lomonova. Design considerations of flux-switching machines with permanent magnet or DC excitation. 15th European Conference of Power Electronics and Applications. 2013. pp. 1-10.

(12) C. H. T. Lee, K. T. Chau, C. Liu, and C. C. Chan. Overview of magnetless brushless machines. IET Electric Power Applications. 2017. DOI: 10.1049/iet-epa.2017.0284.

(13) W. Hua, M. Cheng, Z. Zhu, and D. Howe. Analysis and optimization of back EMF waveform of a flux-switching permanent magnet motor. IEEE Transactions on Energy Conversion. 2008. vol. 23, no. 3, pp. 727-733.

(14) C. H. T. Lee, K. T. Chau, and C. Liu. Design and analysis of an electronic-geared magnetless machine for electric vehicles. Transactions on Industrial Electronics. 2016. vol. 63, no. 11, pp. 6705-6714.

(15) C. H. T. Lee, K. T. Chau, C. Liu and C. C. Chan. Development of a singly fed mechanical-offset machine for electric vehicles. IEEE Transactions on Energy Conversion. 2018. vol. 33, no. 2, pp. 516-525.

(16) J. Chen and Z. Q. Zhu. Winding configurations and optimal stator and rotor pole combination of flux-switching PM brushless AC machines. IEEE Transactions on Energy Conversion. 2010. vol. 25, no. 2, pp. 293-302.

(17) C. H. T. Lee, K. T. Chau, C. Liu, D. Wu, and S. Gao. Quantitative comparison and analysis of magnetless machines with reluctance topologies. IEEE Transactions on Magnetics. 2013. vol. 49, no. 7, pp. 3969-3972.

(18) C. H. T. Lee, K. T. Chau, C. Liu, T. W. Ching, and F. Li. A high-torque magnetless axial-flux doubly salient machine for in-wheel direct drive applications. IEEE Transactions on Magnetics. 2014. vol. 50, no. 11, pp. 8202405:1-5.